



ELSEVIER

Available online at [www.sciencedirect.com](http://www.sciencedirect.com)

SCIENCE @ DIRECT®

Optics Communications 220 (2003) 59–66

OPTICS  
COMMUNICATIONS

[www.elsevier.com/locate/optcom](http://www.elsevier.com/locate/optcom)

## Optical 3D-storage in sol–gel materials with a reading by optical coherence tomography-technique

Jorge-Alejandro Reyes-Esqueda<sup>a,\*</sup>, Laurent Vabre<sup>b,2</sup>, Romain Lecaque<sup>b</sup>, François Ramaz<sup>b</sup>, Benoît C. Forget<sup>b</sup>, Arnaud Dubois<sup>b</sup>, Bernard Briat<sup>b</sup>, Claude Boccara<sup>b</sup>, Gisèle Roger<sup>a</sup>, Michael Canva<sup>a</sup>, Yves Lévy<sup>a</sup>, Frédéric Chaput<sup>c</sup>, Jean-Pierre Boilot<sup>c</sup>

<sup>a</sup> *Groupe d'Optique Non-linéaire, Laboratoire Charles Fabry de l'Institut d'Optique Théorique et Appliquée, CNRS UMR 8501, Ecole Supérieure d'Optique, Bât 503, Université Paris Sud, Orsay Cedex 91403, France*

<sup>b</sup> *Laboratoire d'Optique Physique, CNRS UPR A0005, UPMC, Ecole Supérieure de Physique et de Chimie Industrielles, 10 rue Vauquelin, Paris 75005, France*

<sup>c</sup> *Groupe de Chimie du Solide, Laboratoire de Physique de la Matière Condensée, CNRS UMR 7643, Ecole Polytechnique, Palaiseau Cedex 91128, France*

Received 18 July 2002; received in revised form 28 February 2003; accepted 17 March 2003

### Abstract

We report on the recording of 3D optical memories in sol–gel materials by using a non-linear absorption effect. This effect induces a local change in optical properties of the material which is read and quantified with a high-resolution full-field optical coherence tomography setup. It is the first time that this technique is used for this purpose. Data recording was performed by focused picosecond (ps) single-pulse irradiation at 1064 nm with energy densities of 10 and 33 J/cm<sup>2</sup> per pulse.

© 2003 Elsevier Science B.V. All rights reserved.

PACS: 42.70.M; 42.30.W; 42.70.L; 42.65

**Keywords:** Non-linear materials; Sol–gel; Optical coherence tomography; Optical data storage; Non-linear absorption; Two photon absorption

\* Corresponding author. Present address: Ciudad Universitaria, Instituto de Física, UNAM, Mexico City 04510, Mexico. Tel.: +52-562-25103; fax: +52-561-61535.

E-mail address: [reyes@fisica.unam.mx](mailto:reyes@fisica.unam.mx) (J.-A. Reyes-Esqueda).

<sup>1</sup> Supported by Conacyt (Mexico) and the Ministère de la Recherche (France).

<sup>2</sup> Supported by the Délégation Générale pour l'Armement (France).

### 1. Introduction

In recent years, several strong efforts have been made in order to increase storage computer capability as the limit of the conventional media ( $2.5 \times 10^9$  bits/cm<sup>2</sup> read at  $\lambda = 200$  nm [1]) has almost been reached. The removability, replicability, durability, lightness, and its low cost have

made optical memory more advantageous than magnetic data storage. However, there are some unbreakable physical limits for this kind of memory. One of these barriers, the diffraction of laser light, limits the density of stored information to the inverse of the wavelength used to write raised to the power of the dimensions used to store information ( $\rho \sim 1/\lambda^2$  in two-dimensional systems, where  $\rho$  is the density of information and  $\lambda$  the wavelength). This equation suggests that the information storage is much higher for UV than for IR light, nevertheless the shorter the wavelength, the stronger the Rayleigh scattering inside the medium. Yet, wavelength is not the only parameter that determines the stored data density even if it remains an important one.

Remaining within these borders, the recently available digital versatile disk (DVD) system uses a laser with a shorter wavelength than for compact disc (CD) and also a lens with a larger numerical aperture, which allows a rise of the density storage by a factor of 7.3 [2]. With the intention of fulfilling the increasing demand in the information storage field, several methods to break those density limits have been attempted. Hybrid near-field optics [3] and other three-dimensional (3D) optical recording techniques like optical spectral hole burning [4], holographic data storage [5] and two photon absorption (TPA) [1,6–14] have been recently used in this direction.

In the case of multi-photon absorption, there exists a threshold above which a change in the optical properties may be induced in a reduced volume. This change occurs at the focal point of a laser beam. This fact ensures avoiding cross talk in the writing phase and since TPA depends on the square of the radiation flux intensity, the optical properties will change within a localized volume in the range of  $\lambda^3$ . For an IR laser, an interaction volume of  $1 \mu\text{m}^3$  corresponds to a storage density of  $1 \text{ Tbit}/\text{cm}^3$ . According to the materials' properties, the main physical mechanisms used for recording by TPA are photopolymerization [11], photochromicity [7], dimer–monomer transformation [1], control of the media acidity [1], diffusional redistribution of fluorescent molecules [12] and photobleaching [3,13,14]. Another important recording mechanism indirectly linked to TPA

because of the multi-photon feature of the absorption, is the optical damaging of a material by micro-explosion [15,16] in the region of the focus of laser irradiation.

In the present work, we write binary data by using a focused single laser shot at 1064 nm. The writing mechanism is related to TPA and micro-explosion processes, as it will be shown below. Up to now, crystals [17], silica glasses [15], and more often polymers [3,5,6] have been used for recording 3D structures. To the best of our knowledge, it is the first time that sol–gel materials, either undoped or doped with organic dyes, are being used as storage media.

Concerning the reading process of the data, essentially single- [18], two- [19] and multi-photon [20] techniques have been used. These are mainly based on measurement of fluorescence or transmission from the memory. In a few cases, data have been read through differential interference contrast [11] and confocal microscopies [2]. The technique presented here is quite different and original. By means of optical coherence tomography (OCT) [21], we can select the backscattered light from a particular layer inside the volume of the media, because of the small coherence length of the illuminating light source. Once more, it seems to be the first time that full-field OCT is used for reading information from a 3D optical memory.

We present in this paper original results concerning optical volume storage, where binary data are recorded by using the non-linear properties of hybrid sol–gel samples doped with organic dyes and read with a new and efficient technique. In Section 2, we present the materials used as well as recording and reading setups. Then, in Section 3 we present results and discussion, and finally we give our conclusions.

## 2. Experimental methods

### 2.1. Materials

The method for general synthesis of silica-based doped xerogels has been previously reported [22]. Hydrolysis of organically modified silicon precursors

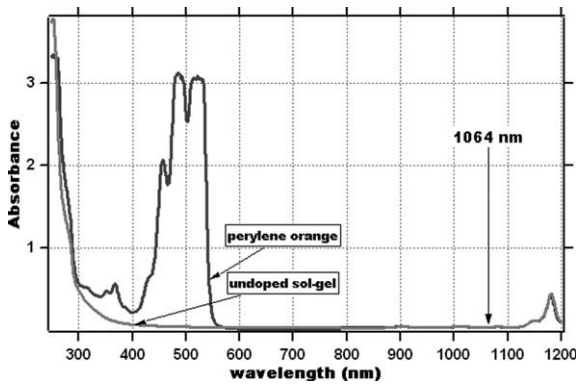


Fig. 1. Linear absorption spectra of undoped and perylene orange-doped sol-gel samples.

sor was performed under acidic conditions with acetone as a common solvent. After several hours of hydrolysis at room temperature, a small amount of amine modified silicon alkoxide was added to neutralize acidity of the medium, thereby increasing the condensation reaction rate. An acetic solution of laser dye was then added to yield a concentration in a range from  $10^{-4}$  to  $10^{-3}$  mol/l. Afterward, the resulting sol was poured into polypropylene cylindrical-shaped molds and sealed. After drying at 70 °C for several weeks, dense monolithic xerogels (30 mm in diameter and 10 mm thick) were obtained. Finally, samples were machined and polished (around 4 nm of roughness). For the purposes of this work, two SiO<sub>2</sub> sol-gel samples, one undoped and one doped were selected to be tested as optical memories. As doping molecule, we chose one molecule from Perylene families, Perylene orange. As it was previously reported, this molecule is sensitive to pulsed irradiation [23]. Moreover, previous results show that its spectroscopic features make it very suitable for TPA with picosecond pulses at 1064 nm [24]. The linear absorption spectra of both samples are shown in Fig. 1.

## 2.2. Recording

The information storage setup is shown schematically in Fig. 2. A Nd:YAG laser emitting 45 picosecond (ps) pulses, at 1064 nm, with a repetition rate of 10 Hz, was used for writing information into the material. Single-shots were obtained

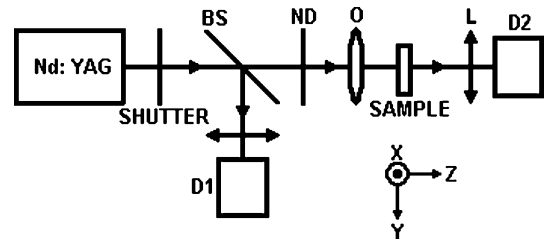


Fig. 2. Experimental system for writing information in 3D. A Nd:YAG 1064 nm ps-pulsed laser. BS, beam splitter; L, lens; ND, neutral optical density; O, microscope objective; D1 and D2, photodiodes.

by using a laser-synchronized shutter. Neutral optical densities were used to control intensity of the incident light during the recording process. The energy densities used for the inscription were 0.1, 0.3, 1, 3.3, 10, 33 and 100 J/cm<sup>2</sup>. In addition, we tuned the total incident energy by controlling the number of incident shots onto the sample. In this way, 1, 2, 4, 8, 16 and 32 single-shots were used to write each single bit. We also used periods of 3, 10 and 30 s of consecutive shots at 10 Hz to write some of the bits. The laser beam was focused into the sample by using a (0.5, 20×) microscope objective. A (x–y–z) translation stage was employed to control the position of the sample. The reference beam (used to take into account the laser intensity fluctuations) and sample transmission signals were focused and then collected onto photodiodes D1 and D2, respectively. The writing step was monitored by measuring the induced decrease in the transmission signal, which indicates non-linear interaction of the laser beam with the medium.

## 2.3. Reading

Photo-induced variations are read in a linear low-flux regime. The main idea is that the localized induced spots backscatter incident light due to the refractive index variation. Reading the spot from a particular layer is achieved with a full-field OCT device [25] as shown in Fig. 3. This setup is a modified Michelson interferometer where each arm contains the same microscope objective (Lin-nik Configuration), with the aim of imaging the sample and a reference mirror. The optical signal

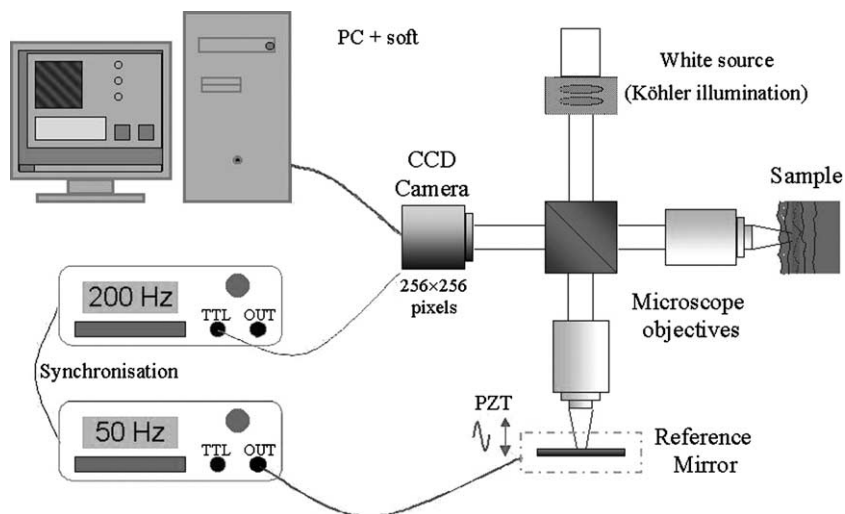


Fig. 3. Schematic representation of our Linnik interference microscope. A piezoelectric transducer induces a phase modulation (50 Hz), which is synchronized to the image acquisition of a CCD camera (200 Hz) by means of two generators.

that we measure is an interference pattern between the backscattered light from a particular layer and the reference beam. For this purpose, we use a DALSA system CCD camera –  $256 \times 256$  pixels 8 bits – working at a maximum rate of  $f = 200$  frames/s. The coherence length of the light source (a 100 W tungsten–halogen lamp) is short; consequently, we can obtain images with an axial resolution ( $z$ ) close to  $1 \mu\text{m}$ . The lateral resolution ( $x, y$ ) of the setup depends upon the numerical aperture of the objectives. We commonly use (0.25,  $10\times$ ) and (0.40,  $20\times$ ) objectives reaching  $\sim 1 \mu\text{m}$  of lateral resolution. In general, the acquisition time is of 1 s.

The interference pattern is sinusoidally modulated by vibration of the reference mirror induced with a piezoelectric transducer. This modulation rates at  $f/4 = 50$  Hz, and it is synchronized to image acquisition of the camera by means of two phase-locked generators. As fully described elsewhere [26], the pixels of the camera are treated in parallel; each image within the sample (corresponding to a path retardation) is the record of a sequence of four acquisitions. The amplitude and phase of the signal are given by linear combinations between these four shifted images. This technique allows a fast parallel-reading scheme, with a very large axial resolution.

### 3. Results and discussion

The bits (data marks) were recorded in two sol–gel samples. Undoped sol–gel and Perylene orange-doped sol–gel matrices were submitted to single laser pulses between  $0.1$  and  $100 \text{ J}/\text{cm}^2$ . The number of pulses was adjusted as indicated in the experimental section, from 1 to 32 single-shots, and from 3 to 30 s of consecutive shots at 10 Hz. This control of the incident energy is shown in Fig. 4 for Perylene orange sol–gel matrix: the minimum energy density necessary for writing into the Perylene orange sample was of  $10 \text{ J}/\text{cm}^2$  with 4 single-shots per bit (point a). There is no trace of recording for lower energies. For the undoped sample, this minimum was of  $33 \text{ J}/\text{cm}^2$  with one single-shot per bit. As it is also seen in the figure, single-shot recording at  $33 \text{ J}/\text{cm}^2$  is possible for Perylene orange sample (point b), indicating the feasibility of systematic single-shot recording with our system. The recording at  $100 \text{ J}/\text{cm}^2$  was detected in a different plane than that shown in the figure. This is due to an effect of self-focusing of the beam, as it will be discussed below.

As it is shown in Figs. 5(a) and (b), by using the energy density of  $33 \text{ J}/\text{cm}^2$ , with 2, 4 and 8 laser pulses per bit (left to right), we recorded two different data pages into the Perylene orange bulk

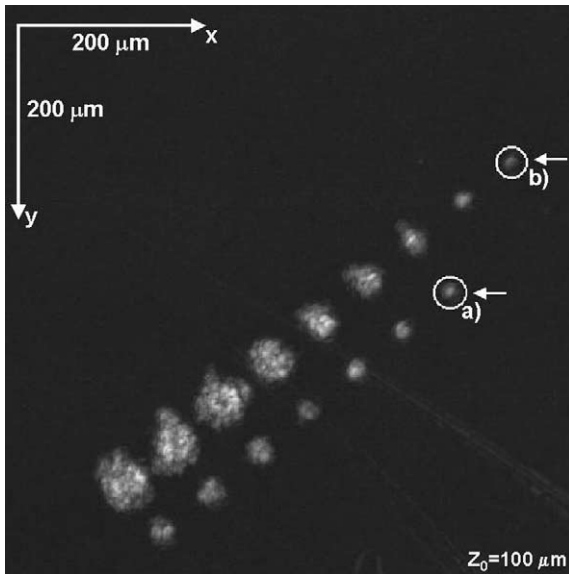


Fig. 4. Control of the incident energy for the Perylene orange sample. For a field of view of  $600 \times 600 \mu\text{m}^2$ , two lines of bits written at  $33$  and  $10 \text{ J/cm}^2$  are shown (upper and lower, respectively). The distance between bits is of  $40 \mu\text{m}$ . Each bit was marked with a different number of pulses, varying from 1 single-shot to 30 s of consecutive shots (from right to left). The minimum energy density necessary to have a bit-mark was of  $10 \text{ J/cm}^2$  with 4 single-shots per bit (the encircled bit marked with letter a; letter b marks a bit recorded with a single-shot at  $33 \text{ J/cm}^2$ ). See Fig. 8 for the arrows.

sample. A distance of  $60 \mu\text{m}$  between the page planes was measured, with the first of them located  $115 \mu\text{m}$  under the surface. Distance between bits was of  $60 \mu\text{m}$ . Fig. 6 shows also the readout signal through a row of 5 bits recorded in the same sample using the minimum energy density of

$10 \text{ J/cm}^2$  with 4 laser pulses per bit. They were separated by a distance of  $20 \mu\text{m}$ , each  $5\text{--}7 \mu\text{m}$  in diameter, with an axial length of  $\sim 10 \mu\text{m}$ . The power-signal to noise ratio was found to be around 140 for an acquisition time of 1 s. This ratio is rather large and may allow a faster acquisition, for example within 100 ms with a resultant power-signal to noise ratio of  $\sim 44$ . These results demonstrate the potential of using dye-doped sol-gels as a medium for 3D optical data storage as well as the prospective of our OCT-based parallel-reading scheme.

We compared the intensity of backscattered signal from data marks to the one obtained from the surface of the sample. Considering a reflection coefficient of 4% for the surface, we deduced an equivalent reflection coefficient of  $R \approx 2.5 \times 10^{-7}$  for the data marks. For the sake of comparison, if we were to assume a uniform effect over the depth of data marks, this equivalent reflection coefficient would correspond, using a classical Fresnel approximation, to an induced refraction index variation of  $\Delta n \approx 8 \times 10^{-4}$  for the recorded bits. Increased  $\Delta n$  would increase the backscattered signal, but one must bear in mind that the signal read from “lower” pages must propagate through the “upper” pages of randomly distributed data marks, which would also scatter the signal, increasing cross talk and affecting device performance. Moreover, an increased refraction index change would arise from a larger induced change into the matrix, which may imply spending more energy in recording, and therefore a more expensive writing system. On another hand, according to

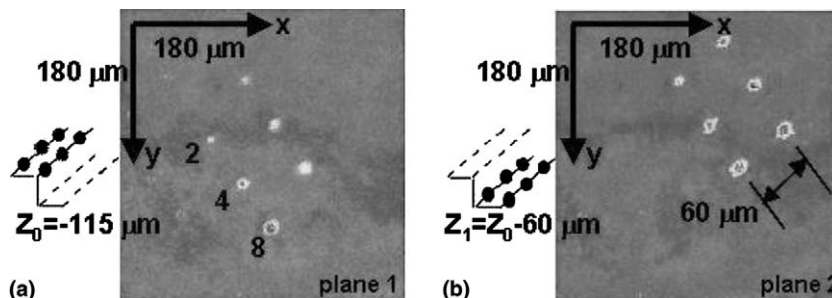


Fig. 5. (a) and (b) show two pages of data separated by  $60 \mu\text{m}$  in the axial direction. The field of view is  $360 \times 360 \mu\text{m}^2$  for an exposure time of 1 s and an  $(0.25, 10\times)$  objective. The distance between bits is of  $60 \mu\text{m}$ .

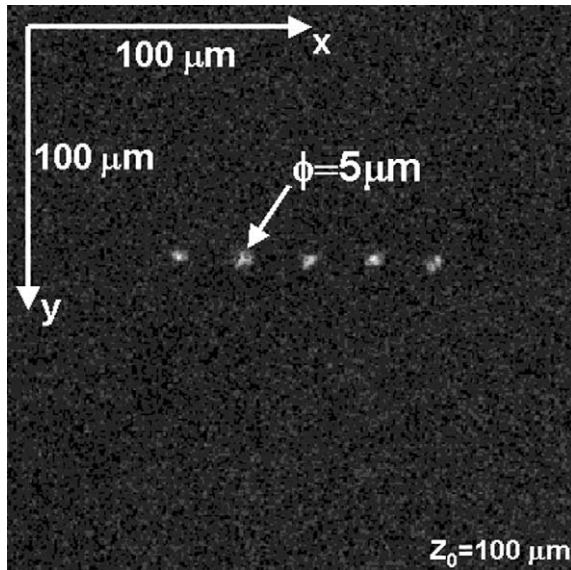


Fig. 6. The readout signal is shown through a row of 5 bits recorded on a plane in the Perylene orange sample at  $10 \text{ J/cm}^2$  with four laser pulses per bit. The field of view is  $200 \times 200 \mu\text{m}^2$  for an (0.40,  $20\times$ ) objective. The distance between bits is of  $20 \mu\text{m}$ .

this evaluation, the sensibility of our new reading device is high enough for the readout of recorded information.

Since recording was also observed in undoped sol-gel matrix, other processes, besides that of TPA of the organic chromophore, must be taken into account (see absorption spectra in Fig. 1). Furthermore, as it is shown in Fig. 7 for the Per-

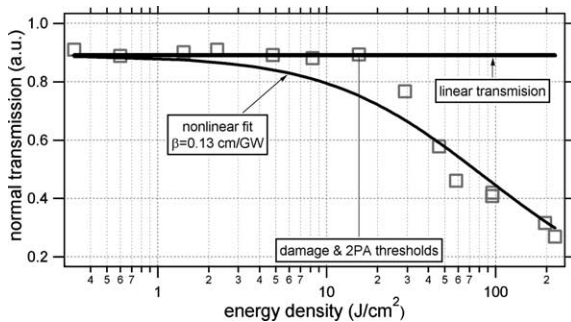


Fig. 7. Limiting curve of the Perylene orange sample showing the superposition of its damage material and TPA thresholds. The non-linear coefficient  $\beta$  was evaluated by fitting the experimental data to the normalized transmission when TPA occurs for a Gaussian beam.

ylene orange sample, within its optical limiting curve, the material optical damage and TPA energy thresholds are very close. This result was also observed in other differently doped sol-gel materials, particularly when doping with rhodamine and pyrromethene families. This was even observed for a conventional  $\text{SiO}_2$  glass sample.

These results may be explained by considering multi-photon absorption, thermal effects and dielectric breakdown. In particular [27] is very relevant showing the possible interaction of all these different phenomena into the 3D single-pulse micro-modification of transparent materials. Results in the literature show the possibility of recording in these materials by generating ultrafast-laser micro-explosions [16,28]. The energy deposition is initiated by multi-photon absorption [27,29,30] leading to stationary thermal lensing [31], which initiates a strong self-focusing of the beam [29,32], even if it is already externally and tightly focused. As a consequence of this self-focusing, a hot, high-density electron plasma is produced transferring its excess energy to the lattice by electron-phonon coupling [27,29,32,33].

This plasma energy transfer has a lifetime (strongly dependent on the pulse energy) ranging between 10 and 70 ps [32]. This is the reason why, in the case of femtosecond (fs) pulses, the bits recorded are very small heat-affected zones [29,33] and therefore smaller than those recorded in picosecond regime, where energy transfer occurs during the pulse application itself, resulting larger and irregularly shaped structures that display radially extending cracks [28].

Since we used a picosecond regime, it was normal to observe this plasma (a white flash inside of the sample) in both of our samples at the moment of delivering the pulse, then inducing the observed irregularity of the backscattered readout signal over the profile of the two encircled bites, (a) and (b), showed in Fig. 4. This profile is shown in Fig. 8 and is seen from the lateral point of view of the arrows in Fig. 4 and integrated over circles' diameter.

Otherwise, it has also been suggested that this measured index variation implies that micro-explosions create voids in the material, and then a compaction of the surrounding region [29,30].

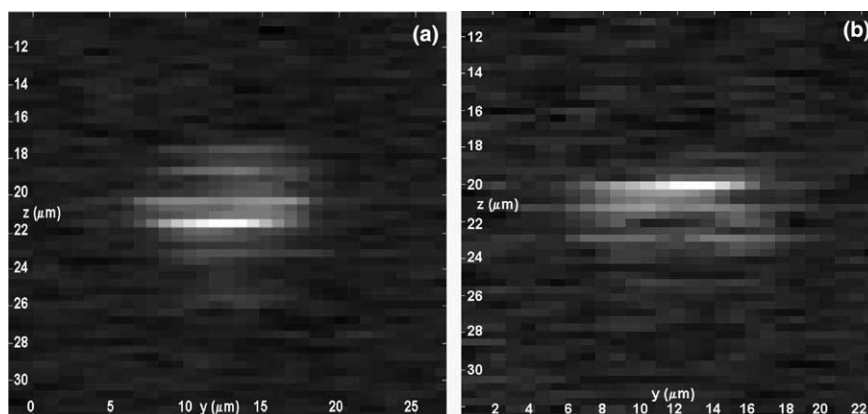


Fig. 8. Transversal view of Fig. 3 from the lateral point of view of the arrows and integrated between the circles' diameter (a) and (b). The irregularity of the backscattered readout signal can be seen over the profile of the two encircled bites showed in Fig. 4.

As well, the recording threshold difference for undoped and doped samples suggests a molecular effect. This may imply a pure molecular TPA besides a matrix multi-photon absorption leading to a micro-explosion recording, as mentioned above. Therefore, additional experiments are being performed with our system in order to elucidate the recording mechanism into undoped and doped sol-gel materials. These experiments include the use of better chromophores with higher TPA-cross-sections, molecular concentration control by binding the molecules to the sol-gel matrix, spatial filtering of the laser beam (since the actual bit spot size is very sensitive to the spatial mode of irradiation pulses, especially for energy into these limits [15]) and fs-recording.

#### 4. Conclusions

Volumic data recording and reading have been performed for the first time into undoped and doped sol-gel thick materials. Recording used 1064 nm picosecond optical pulses. The energy threshold was found to be 33 and 10 J/cm<sup>2</sup> for undoped and perylene-doped sol-gel samples, respectively. A new efficient parallel-reading system based on a full-field OCT-technique has been proposed. We have shown the possibility of 3D optical storage in sol-gel materials with a reading in parallel. The experimental results show the

potentiality of our system for this kind of application, although further research is needed in order to better understand the recording mechanism and to improve it.

#### Acknowledgements

This work has been supported by a grant coming for the ACI-Photonics project from the Ministère de la Recherche (France). J.A. Reyes-Esqueda acknowledges Conacyt (Mexico) and the Ministère de la Recherche (France) for their support for a postdoctoral scholarship. L. Vabre acknowledges the Délégation Générale pour l'Armement (France) for its support.

#### References

- [1] A.S. Dvornikov et al., IEEE Transactions on Components, Packaging, and Manufacturing Technology, Part A 20 (2) (1997) 203.
- [2] S. Kawata, Proc. IEEE 87 (12) (1999) 2009.
- [3] Y. Shen et al., Opt. Commun. 200 (1–6) (2001) 9.
- [4] W.E. Moerner, Persistent Spectral Hole-Burning: Science and Applications, Springer, Berlin, West Germany, 1988.
- [5] S. Orlic, S. Ulm, H.J. Eichler, J. Opt. A 3 (2001) 72.
- [6] F. Charra et al., Proc. SPIE 2042 (1994) 333.
- [7] S. Hunter et al., Opt. Memory Neural Networks 3 (2) (1994) 151.
- [8] A.S. Dvornikov, P.M. Rentzepis, Opt. Commun. 119 (3–4) (1995) 341.

- [9] F.B. McCormick et al., Proc. SPIE 2604 (1996) 23.
- [10] Z. Haichuan et al., Proc. SPIE 4089 (2000) 126.
- [11] J.H. Strickler, W.W. Webb, Opt. Lett. 16 (22) (1991) 1780.
- [12] M.M. Wang, S.C. Esener, Appl. Opt. 39 (11) (2000) 1826.
- [13] A. Shih, S.J. Pan, W.S. Liou, M.S. Park, J. Bhawalkar, J. Swiatkiewicz, P. Prasad, P.C. Cheng, Cell Vis. 4 (2) (1997) 223.
- [14] M. Gu, D. Day, Opt. Lett. 24 (5) (1999) 288.
- [15] M. Watanabe et al., Jpn. J. Appl. Phys., Part 2 (Letters) 37 (12B) (1998) L1527.
- [16] K. Yamasaki et al., Appl. Phys. Lett. 76 (8) (2000) 1000.
- [17] Y. Kawata, H. Ishitobi, S. Kawata, Opt. Lett. 23 (10) (1998) 756.
- [18] H.E. Pudavar et al., Appl. Phys. Lett. 74 (9) (1999) 1338.
- [19] M. Watanabe et al., Appl. Phys. Lett. 77 (1) (2000) 13.
- [20] Y. Kawata, C. Xu, W. Denk, J. Appl. Phys. 85 (3) (1999) 1294.
- [21] D. Huang et al., Science 254 (5035) (1991) 1178.
- [22] M. Faloss et al., Appl. Opt. 36 (27) (1997) 6760.
- [23] A. Dubois et al., Appl. Opt. 35 (18) (1996) 3193.
- [24] M. Canva et al., Opt. Mater. 18 (4) (2002) 391.
- [25] L. Vabre, A. Dubois, A.C. Boccara, Opt. Lett. 27 (7) (2002) 530.
- [26] A. Dubois et al., Appl. Opt. 41 (4) (2002) 805.
- [27] N. Biturin, A. Kuznetsov, J. Appl. Phys. 93 (3) (2003) 1567.
- [28] E.N. Glezer et al., Opt. Lett. 21 (24) (1996) 2023.
- [29] E.N. Glezer, E. Mazur, Appl. Phys. Lett. 71 (7) (1997) 882.
- [30] D. Day, M. Gu, Appl. Phys. Lett. 80 (13) (2002) 2404.
- [31] S.M. Mian, S.B. McGee, N. Melikechi, Opt. Commun. 207 (2002) 339.
- [32] S.-H. Cho, H. Kumagai, K. Midorikawa, Opt. Commun. 207 (2002) 243.
- [33] R. Le Harzic, N. Huot, E. Audouard, C. Jonin, P. Laporte, Appl. Phys. Lett. 80 (21) (2002) 3886.